

## A Robot-Assisted Finishing System with an Active Torque Controller

Y.T. Wang and Y.J. Jan

Department of Mechanical Engineering, Tamkang University  
151 Ying-Chuan Rd., Tamsui, Taipei, Taiwan 25137  
ytwang@mail.tku.edu.tw

### Abstract

*The development of a robot-assisted surface finishing system with an active torque controller is presented in this paper. We utilize a dexterous manipulator to attain the desired position and orientation in three-dimensional space during finishing processes. A single-axis active controller consists of a dc motor and a software observer is attached to the robot wrist and used to actuate a pneumatic hand-grinder. The torque observer is designed to sense the grinding contact force based on the driving current and output position of the motor. The function of the active torque controller includes observing the polishing contact force, applying a desired polishing pressure in the normal direction of the specimen surface, and adjusting the contact angle between the hand-grinder and the surface of the workpiece. In this research, the prototype of a robot-assisted finishing system is constructed and tested on a Tatung A530 robot. The experimental results show that the robot-assisted finishing system functions well under a variety of grinding and polishing conditions.*

### 1. Introduction

Grinding and polishing processes are time-consuming and monotonous operations which strongly rely on skilled human-workers. To automate these processes and achieve desired surface roughness, it is important to control the grinding path, feed rate, grinding-wheel speed, contact force and cutting depth. Among them, to generate a suitable tool-path and to control the contact force are two major challenge issues. For example, to polish free-form surfaces of an object requires a delicate machine to follow complicated polishing paths. In this case, a polishing system based on a robot manipulator is more effective than that on a NC machining center in order to follow the curved free-form surfaces. On the other hand, during finishing operations, the tool comes into physical contact with the workpiece and causes contact forces between them. It is difficult to control these contact forces which depend on the cutting depth, feed rate, grinding-wheel speed and material properties.

Many researchers have proposed automated systems for polishing of dies, deburring of castings, and removing of weld beans etc [4-7,10]. Usually, a polishing tool is

mounted on a NC machining center or a robot manipulator and a multi-dimensional force sensor is included in the system to improve finishing accuracy. It is troublesome to handle the multi-dimensional force control system in run-time processes, besides the passive-type force sensors are expensive in price and sensitive to a noise.

We propose an automated finishing system for polishing a free-form surface using an active torque controller mounted on the end-effector of an industrial robot. To simplify the force-control action, only the contact force normal to the polishing surface is concerned and a software-type torque observer is used to replace the role of a hardware sensor.

### 2. Polishing robot system

The developed robot-assisted surface finishing system consists of a 5-axis articulated industrial robot, an end-effector, a robot controller, a xy-table for setting the metal mold, and a personal computer for sensory processing essential to a contact force control. The system configuration is shown as Figure 1. The system utilizes a dexterous manipulator, Tatung A530, to attain the desired position and orientation of the end-effector in three-dimensional space. A dc motor is attached to the robot wrist and used to actuate the polishing tool. The torque observer is designed to sense the applied torque based on the driving current and output position of the dc motor. A pneumatic hand-grinder is serially mounted on the observer-motor. We control the motion and contact force of the hand-grinder to perform the desired finishing action. The robot follows a desired tool path and drives the hand-grinder to come in contact with the workpiece. The single-axis torque observer can sense the contact force and direct the hand-grinder to apply a desired contact pressure on the workpiece. The kinematic analysis and a torque control algorithm for the torque observer are derived in the following sections.

### 3. Kinematic analysis

In order to polish a workpiece with free-form surfaces, a 7-d.o.f. mobility is provided by the finishing system formed by a Tatung A530 robot and a xy-table as shown in Figure 2. The workpiece is placed on the xy-table. During the process, the manipulator drives the polishing tool to

follow a programmed path and attain a desired orientation. Three rotational angles and the position in z-axis are performed by the A530 robot. Positions in x- and y-axis are driven by the xy-table. The Denavit-Hartenberg parameters of the A530 manipulator are listed in Table 1. There is one more d.o.f. mobility provided by the DC observer-motor. We control the current command and the angular position of the motor in order to ensure that the tool is kept at a desired contact angle and contact pressure with the workpiece. Usually, the contact angle,  $\theta_f$ , is measured from the surface at contact point in the drive-feed direction as shown in Figure 3.

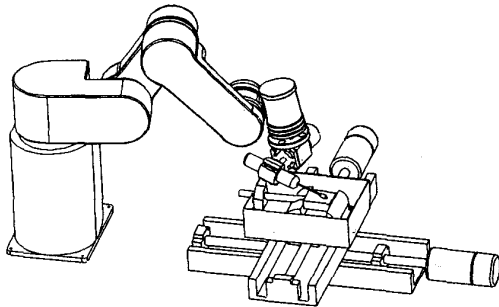


Figure 1 Polishing Robot System

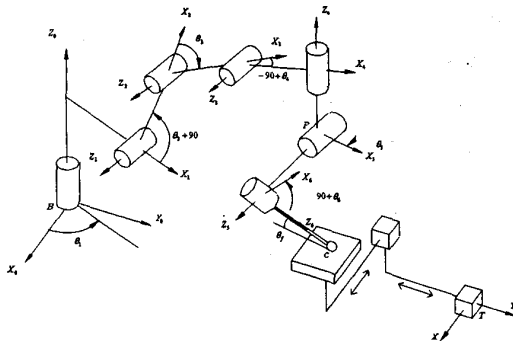


Figure 2 Coordinate systems of the polishing system

Table 1 DH parameters of the A530 manipulator (in mm)

$i$	$a_i$	$\alpha_i$	$d_i$	$\theta_i$
1	160	90	330	$\theta_1$
2	200	0	0	$90+\theta_2$
3	240	0	0	$\theta_3$
4	80	-90	0	$-90+\theta_4$
5	0	0	-85	$180+\theta_5$

Assume that the contact angle is retained at a magnitude of  $\theta_f$ , and the contact at point  $C$  is a point contact, then the homogenous transformation matrix from the robot-base coordinate,  $B$ , to the coordinate of the contact point,  $C$ , can be expressed as

$$A_C^B = A_T^B A_C^T = A_P^B A_C^P$$

where  $T$  and  $P$  are located at the coordinate origins of the base of the xy-table and the robot end-effector,

respectively. During the finishing process, the desired position coordinate of the contact point  $C$  and the orientation of the tool relative to surfaces of the specimen are generated. The transformation from the robot-base frame to the end-effector is determined by

$$A_P^B = A_T^B A_C^T (A_C^P)^{-1} = A_C^B (A_C^P)^{-1} \quad (1)$$

where  $A_C^P$  could be found by the knowledge of  $\theta_f$  and tool length. From Equation (1), we can find the desired joint angles of A530 robot by an inverse kinematic method. These joint angles are the inputs of the robot motion controller.

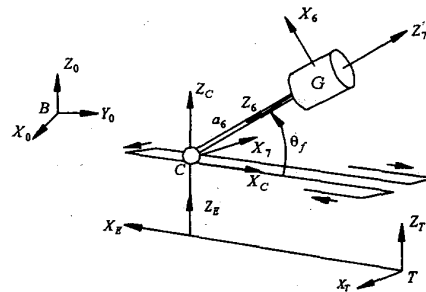


Figure 3 Coordinate systems for the contact area

#### 4. Polishing Path

A typical curved surface of a specimen is shown in Figure 4. We can formulate different types of tool path for the robot to perform a task on this workpiece. Two types of tool path, zigzag and fractal, are used in this research for comparison. A zigzag is a path with repeated switching of directions from drive-feed to its perpendicularity, as shown in Figure 5. A fractal tool path is generated based on the Hilbert "□" pattern. A L-system method [3] using logical symbols is adopted here to generate the Hilbert "□" pattern. Definitions of the logical symbols are stated as following:

F: Drawing a fixed-length line from current position to new position

-: turning an angle of  $90^\circ$  in CCW direction

+: turning an angle of  $90^\circ$  in clockwise direction

L: +F-F-F+

R: -F+F-F-

Generation rules of the Hilbert curve are: (a) substituting "+RF-LFL-FR+" into L, "-LF+RFR+FL-" into R when the order increases, (b) repeating the processes in every increment of order, and (c) the zero-order starting from the L-operation.

Figure 6 depicts a 2<sup>nd</sup>-order fractal tool path based on the generation rules. We found that the fractal path has an advantage of consistency in direction [3].

#### 5. Contact torque control

In the finishing process, an incorrect CAD data or tool wear will cause a contour error. In this case, a pure

position controller could drive the tool to be no contact with or over-cut the workpiece. A suitable torque controller is always needed in a finishing process. In this research, we propose to control only the contact pressure normal to the contact surface. Then the torque controller could be simplified and decoupled from the robot motion controller.

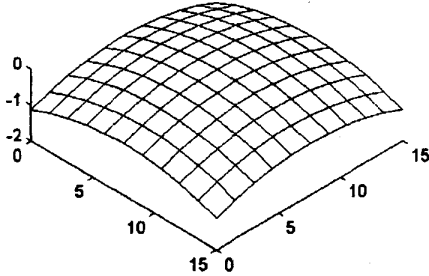


Figure 4 Workpiece with curved surface

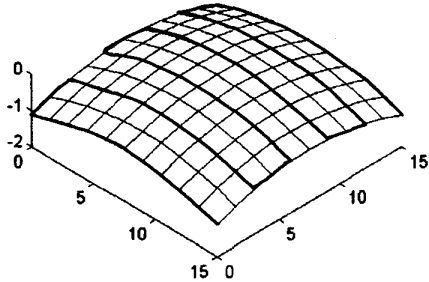


Figure 5 Zigzag tool path

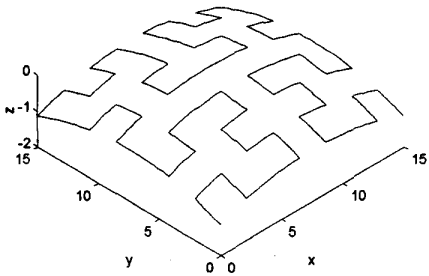


Figure 6 2<sup>nd</sup>-order fractal tool path

We model the contact behavior between the tool and the specimen as a linear rotational spring in Figure 7,

$$T_f = k_e \theta \quad (2)$$

where  $T_f$  is the torque exerted by the observer motor on the surface of the workpiece;  $k_e$  is the rotational spring constant;  $\theta$  is the angular displacement of the motor. The dynamic equation of the end-effector system with an observer motor and a hand-grinder can be expressed as

$$T_{em} = J\ddot{\theta} + k_e\theta + T_L \quad (3)$$

where  $T_{em}$  and  $T_L$  are the applied torque and external load, respectively.  $J$  is the inertia of the system. From Equation (2), we have

$$\theta = k_e^{-1} T_f$$

$$\ddot{\theta} = k_e^{-1} \ddot{T}_f$$

Equation (3) can be rewritten as the following equation with the new variable  $T_f$ ,

$$T_{em} = Jk_e^{-1} \ddot{T}_f + T_f + T_L \quad (4)$$

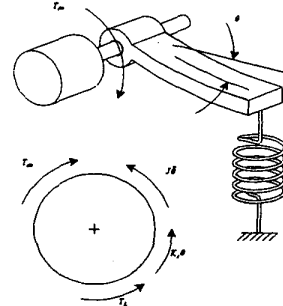


Figure 7 Linear spring model

In order to control the applied torque, a proportional-integral-derivative (PID) controller is considered

$$T_{em} = Jk_e^{-1} [\ddot{T}^* + k_{fp}e_f + k_{fi} \int e_f dt + k_{fd}\dot{e}_f] + T_f + T_L \quad (5)$$

where  $T^*$  denotes the torque command;  $e_f$  is the torque error,  $e_f = T^* - T_f$ ;  $k_{fp}$ ,  $k_{fi}$  and  $k_{fd}$  are the gain values of the PID controller. In this case,  $T_L$  is not suitable to be put in the controller because it is not easy to be measured on-line. The term  $(T_f + T_L)$  in Equation (5)

is replaced by a feed-forward command  $T^*$ . The resultant controller is a PID-plus-feedforward (PIDFF) controller,

$$T_{em} = Jk_e^{-1} [\ddot{T}^* + k_{fp}e_f + k_{fi} \int e_f dt + k_{fd}\dot{e}_f] + T^* \quad (6)$$

The block diagram of the PIDFF controller is shown in Figure 8. Where  $k_t$  is the torque constant of the motor;  $\hat{J}$ ,  $\hat{k}_e$  and  $\hat{k}_b$  are the estimated values of the system parameters  $J$ ,  $k_e$  and  $k_b$ , respectively. In the feedback loop, we replace  $sT_f$  by  $k_e\omega$  in order to reduce the signal noise to the controller. Where  $\omega$  is the angular speed of the motor. In the finishing processes, the contact torque will be kept at a constant value, i.e.  $\dot{T}^* = \ddot{T}^* = 0$ . From Equations (4) and (6), we find the error equation,

$$\ddot{e}_f + k_{fd}\dot{e}_f + \frac{e_f}{Jk_e^{-1}} + k_{fi} \int e_f dt = T_L$$

$$\ddot{e}_f + k_{fd}\dot{e}_f + k_{fp}e_f + k_{fi} \int e_f dt = \dot{T}_L \quad (7)$$

We can see that the value of the steady-state error vanishes as time approaches infinity. If the estimated values of the system parameters are correct, we can derive the transfer function which represents the relationship between the output torque,  $T_f$ , and the command torque,

$$T^*$$

$$\frac{T_f}{T^*} = \frac{(Jk_{fp} + k_e)s + Jk_{fi}}{Js^3 + Jk_{fd}s^2 + (Jk_{fp} + k_e)s + Jk_{fi}} \quad (8)$$

In the case of no disturbance, the output will track the command exactly at steady state, as we can see from Equations (7) and (8). If there exists a disturbance,  $T_L$ , the steady-state error will disappear as time approaches infinity. The PIDFF controller provides a solution to the torque control problem during the finishing process. The analytical and experimental works in this paper are based on the concept of the PIDFF controller.

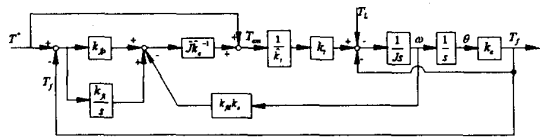


Figure 8 Block diagram of the PIDFF controller

The control algorithm in Figures 8 is used to control the contact torque exerted by the observer motor. As shown in Figure 9, the normal contact force  $F$  at point  $C$  can be determined by dividing the contact torque by the radius  $a_6 = \overline{AC}$ ,

$$F = \frac{T_f}{a_6} \cos \beta$$

Where we can see that  $a_6$  is the length between the center of motor-axis  $A$  and the contact point  $C$ ;  $\beta$  is the angle between  $a_6$  and the surface. The values of  $a_6$  and  $\beta$  can be determined by the following equations,

$$a_6 = \sqrt{r^2 + (a_6' - r)^2 + 2r(a_6' - r)\sin\theta_f}$$

$$\beta = 90^\circ - \cos^{-1} \frac{r^2 + a_6'^2 - a_6^2}{2ra_6}$$

Where  $r$  is the radius of the spherical tool head;  $a_6'$  is the length between point  $A$  and the tool tip, point  $C'$ .

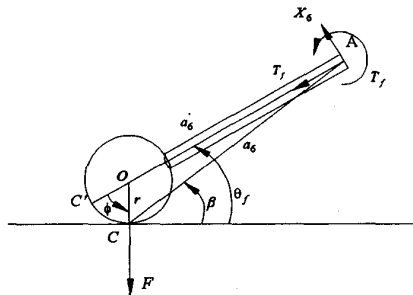


Figure 9 Contact geometry

## 6. Torque observer

We utilize a torque observer to estimate the contact torque during the finishing processes. The torque observer is a linear Luenberger observer [8] as shown in Figure 10. The block diagram is composed of two parts: the upper loop is

the motor system with a torque controller and the lower one is the torque observer. The torque observer estimates the contact torque based on the information of the torque command and the output position of the system.

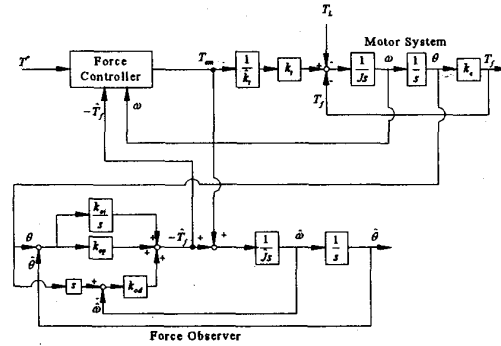


Figure 10 Torque controller with a Luenberger observer

According to Figure 10, the observed torque can be determined as

$$\hat{T}_f = \frac{\hat{k}_t (k_{od}s^2 + k_{op}s + k_{oi})}{\hat{J}s^3 + k_{od}s^2 + k_{op}s + k_{oi}} T_f + \frac{\hat{J}(k_{od}s^3 + k_{op}s^2 + k_{oi}s)}{\hat{J}s^3 + k_{od}s^2 + k_{op}s + k_{oi}} \left[ \left( \frac{\hat{J}\hat{k}_t}{\hat{J}\hat{k}_t} - 1 \right) \omega \right] \quad (9)$$

Where  $k_{op}$ ,  $k_{oi}$  and  $k_{od}$  are gains of the observer. If the parameters,  $\hat{k}_t$  and  $\hat{J}$ , are correctly estimated, Equation (9) can be simplified as

$$\frac{\hat{T}_f}{T_f} = \frac{(k_{od}s^2 + k_{op}s + k_{oi})}{\hat{J}s^3 + k_{od}s^2 + k_{op}s + k_{oi}} \quad (10)$$

In steady state, the torque observer can sense the contact torque exactly.

## 7. Torque Observer Specification

The parameters of the DC observer-motor system are listed in Table 3. The controller is equipped with a PCL-726 D/A interface card and a PCL-833 encoder card by Advantech [1,2]. The D/A card has a 12-bits resolution to represent the output current in the range of  $\pm 5A$ . The basic unit of the current command of the motor drive is calculated as

$$10A \times \frac{1}{2^{12}} = \frac{10}{4095} \cong 2.44 \text{ mA}$$

The resolution of the observer is

$$T = i \times k_t = 2.44 \text{ mA} \times 0.185 \frac{\text{N} \cdot \text{m}}{\text{Amp}}$$

$$= 0.4514 \text{ mN} \cdot \text{m} \times \frac{1 \text{ kgf}}{9.81 \text{ N}} \cong 4.601 \times 10^{-2} \text{ kgf} \cdot \text{mm}$$

The radius between the motor axis and the contact point is  $95 \text{ mm}$ . Then, the resolution of the applied pressure is

$$4.601 \times 10^{-2} / 95 \text{ mm} = 0.48 \text{ gf}$$

This is the smallest force can be applied by the active torque controller. On the other hand, the maximum output-torque is limited by the rate-current of the motor which value is 1 ampere in this case. The maximum output torque can be generated by the controller is determined as

$$T = 0.185 \frac{N \cdot m}{Amp} \times 1 Amp \times \frac{1 kgf}{9.81 N} \times \frac{1000 mm}{1 m} \cong 189 kgf \cdot mm$$

which is about 199 gf for this system.

Table 3 Parameters of the observer-motor

Rated Power	60Watt
Rated Voltage	75V
Rated Current	1.2A
Torque Constant	0.185N·m/A
Rotor Inertia	$1.72656 \times 10^{-3} kg \cdot m^2$
Weight	0.8kgf

### 8. Contact torque Observation

In a finishing process, if the actual motion path differs from the desired one, the contact force at the tip of the polishing tool would not agree with the desired contact force in the transient response. We can measure this deviation of contact torques by using the Luenberger torque observer. The experimental setup is shown as Figure 11. The observer-motor tracks the surface horizontally and goes over the specimen with a step-raise of 10mm in height. The horizontal motion is controlled by a PID position-loop with a damping ratio of 1 and a natural frequency of 50rad/sec. That is,

$$\zeta=1, \quad \omega_n=50 \text{ rad/sec}$$

The gains of the PID controller can be determined as [9]

$$k_p = 0.6865; \quad k_i = 0.01144; \quad k_d = 13.7302$$

The contact stiffness,  $k_e$ , of the metal probe in Figure 11 is 7.44Nm/rad. The observed contact torque,  $T_{ob}$ , is shown in Figure 12. We can see that the step-raise of the tool-path will result in an increase of contact torque.

### 9. Polishing Torque Control

In this example, we control the finishing robot to move in a straight-line path. The observer-motor with a pneumatic hand-grinder is equipped on the wrist of the robot. To simulate the deviation of polishing contour, we put a step-raise of 10mm in the straight-line path. The hand-grinder is driven to cross over the step-arise, while the contact torque is retained at a constant value of 0.12Nm. We utilize the proposed PIDFF algorithm for the control system and a point-to-point motion control for the robot system. The experimental setup is shown as Figure 11. The estimated inertia and contact stiffness of the motor and metal-probe system are  $\hat{J}=0.0013kgm^2$  and  $\hat{k}_e=7.44Nm/rad$ , respectively. The gains of the torque controller and observer are

$$k_{fp}=118.558; \quad k_{fi}=98716.9; \quad k_{fd}=77.0747$$

$$k_{op}=16.9582; \quad k_{oi}=326.523; \quad k_{od}=0.4212$$

The control action during a finishing process is simulated by using Matlab/Simulink, while the experimental work is tested on a Tatum A530 robot. The simulation and experimental results are plotted in Figure 13, where the values of  $sim.T_f$  and  $exp.T_f$  denote the simulation and experimental torques, respectively. The desired torque is controlled at a fixed value of 0.12Nm.

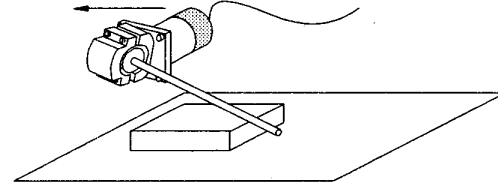


Figure 11 Physical setup of the torque observer with a metal probe

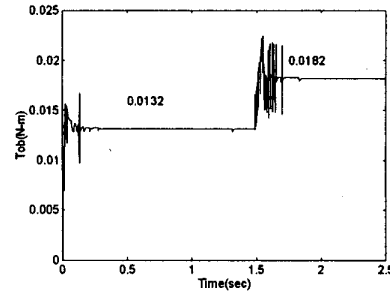


Figure 12 Observed torque versus time

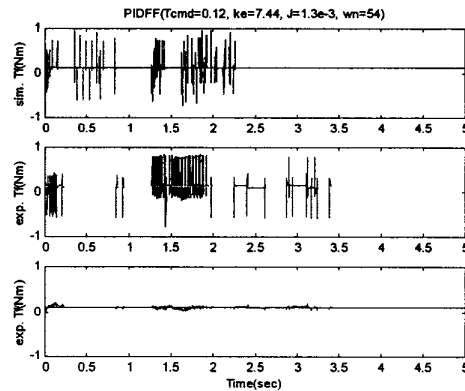


Figure 13 Simulation and experimental values of torques versus time

We can see from the first two plots in Figure 13, the measured torque is corrupted by noise. A first-order low-pass filter in Figure 14 is designed to eliminate the noise. Where  $\tau$  is time constant of the filter;  $K$  is gain of the filter;  $t$  is the sampling time of the digital control system. The filtered torque  $\tilde{T}_f$  at the present time step  $k$  is determined by

$$\tilde{T}_f(k) = \frac{K}{\tau} \hat{T}_f(k) + e^{-\frac{1}{\tau}t} \tilde{T}_f(k-1)$$

The low-pass filter used in this experiment has a cut-off frequency of 10Hz and a gain  $K=1030$ . The filtered torque is depicted as the third plot in Figure 13. The sampling time of the control system is 0.001sec.

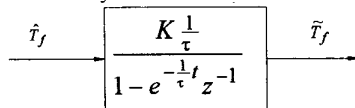


Figure 14 Low-pass filter

### 10. Polishing Robot System

The integrated robot-assisted finishing system is shown in Figure 15. The system includes a Tatum A530 robot for implementing the position and orientation of finishing processes. The torque observer is a 60watt dc motor which is serial-connected to the wrist of the robot. The pneumatic hand-grinder is equipped at the front end of the torque observer. The motion of the manipulator is controlled by a single-board controller. The estimated inertia and contact stiffness of the hand-grinder system are

$$\hat{J} \cong 0.0011 \text{ kg m}^2$$

$$\hat{k}_e = 11.95 \text{ Nm / rad}$$

The gains of the controller and observer are given as

$$k_{fp} = 299.3636; k_{fi} = 226981; k_{fd} = 183$$

$$k_{op} = 5.28; k_{oi} = 70.4; k_{od} = 0.132$$

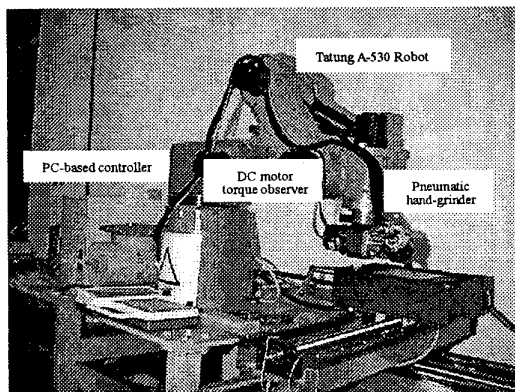


Figure 15 Automated Surface Finishing System

### 11. Conclusions

This paper presents the development of a robot-assisted surface finishing system with an active torque controller. This system utilizes a dexterous manipulator to attain the desired position and orientation of finishing processes in three-dimensional space. A torque observer is attached to the tool frame of the robot manipulator, and a pneumatic hand-grinder is serially mounted on the observer. The function of the active torque controller in the system includes observing the contact torque, applying a desired contact pressure in the

normal direction of the workpiece surface, and adjusting the contact angle between the hand-grinder and the surface of the workpiece. In this research, we construct the prototype of a robot-assisted finishing system. The performance of the torque observer and controller are simulated by using Matlab/Simulink. The software and hardware of the torque control system are tested on a Tatum A530 robot, and the integrated system is used to polish a workpiece with free-form surfaces. The experimental results show that the developed torque observer and controller system functions well under a variety of grinding and polishing conditions. We conclude that the developed finishing robot system has the capability to finish specimens with free-form surfaces.

### Acknowledgement

This work was supported by the National Science Council in Taiwan under grant no. NSC88-2212-E-032-014.

### References

- [1] Advantech, 1994a, PCL-726 six-channel D/A output card user's manual.
- [2] Advantech, 1994b, PCL-833 3-axis quadrature encoder and counter card user's manual.
- [3] Chen, A.C.-C., K.C. Tai, C.H. Chen, Y.C. Wang, P.H. Lo, and Y.T. Wang, 1998, Generation of Fractal Tool Paths for Automated Surface Finishing Processes, Pacific Conference on Manufacturing, Brisbane, Australia.
- [4] Furukawa, T., D.C. Rye, M.W.M.G. Dissanayake, and A.J. Barratt, 1996, Automated polishing of an unknown three-dimensional surface, Robotics & Computer-Integrated Manufacturing, Vol.12, No.3, pp.261-270.
- [5] Jenkins, H.E. and T.R. Kurfess, 1996, Design of A Robust Controller for A Grinding System, IEEE Transactions on Control Systems Technology, Vol. 4, No.1, pp.40-48.
- [6] Kunieda, M., T. Nakagawa, and T. Higuchi, 1984, Development of a Polishing Robot for Free Form Surface, Proceedings of the 5<sup>th</sup> International Conference on Production Engineering, pp.265-270, Tokyo.
- [7] Kurfess, T.R., D.E. Whitney, and M.L. Brown, 1988, Verification of a dynamic grinding model, Journal of Dynamic systems, Measurement and Control, Vol.110, n4, pp.403-409.
- [8] Luenberger, D.G., 1971, An Introduction to Observers, IEEE Transactions on automatic control, Vol. AC-16, No. 6, pp.596-602.
- [9] Perdikaris, G.A. and K.V. VanPatten, 1982, Computer Schemes for Modeling, Tuning, and Control of DC Motor Drive Systems, Proceedings of the Power Electronics International Conference, pp.83-96.
- [10] Takeuchi, Y. and D.-F. Ge, 1992, Generation of polished-sculptured surfaces by advanced machining center-robot complex, Proceeding of the IEEE International Conference on Robotics and Automation, pp.1126-1131.